Enhanced Tropical Eastern Indian Ocean Rainfall Breaks Down the Tropical Easterly Jet–Indian Rainfall Relationship

SIHUA HUANG,[a] BIN WANG,[b,c] ZHIPING WEN,[d,e,f] AND ZESHENG CHEN[g,h]

[a] *Center for Monsoon and Environment Research and School of Atmospheric Sciences, Sun Yat-sen University, Guangzhou, China*
[b] *Department of Atmospheric Sciences and International Pacific Research Center, University of Hawai'i at Mānoa, Honolulu, Hawaii*
[c] *Earth System Modeling Center, Nanjing University of Information Science and Technology, Nanjing, China*
[d] *Department of Atmospheric and Oceanic Sciences and Institute of Atmospheric Sciences, Fudan University, Shanghai, China*
[e] *Innovation Center of Ocean and Atmosphere System, Zhuhai, China*
[f] *Jiangsu Collaborative Innovation Center for Climate Change, Nanjing, China*
[g] *State Key Laboratory of Tropical Oceanography (South China Sea Institute of Oceanology, Chinese Academy of Sciences), Guangzhou, China*
[h] *Southern Marine Science and Engineering Guangdong Laboratory, Guangzhou, China*

(Manuscript received 9 August 2020, in final form 2 December 2020)

ABSTRACT: Previous studies found a tight connection between the tropical easterly jet (TEJ) and Indian summer monsoon rainfall (ISMR). Here we show that the TEJ–ISMR relationship is nonstationary and breaks down from 1994 to 2003 (epoch P2), in contrast to the significant positive correlation during epochs P1 (1979–93) and P3 (2004–16). The breakdown of the TEJ–ISMR relationship concurs with the increased rainfall variability over the tropical eastern Indian Ocean (TEIO). The enhanced TEIO rainfall anomalies excite a significant lower-level cyclonic circulation that reduces the ISMR and meanwhile strengthen the upper-level divergence and excite a pair of upper-level anticyclones to the west of the TEIO as Rossby wave responses, both accelerating the TEJ. Thus, the TEIO rainfall plays a more important role than the ISMR in TEJ variability during P2, causing the breakdown of the TEJ–ISMR relationship. In contrast, a relatively weak amplitude of the TEIO rainfall during P1 and P3 was unable to change the positive TEJ–ISMR relationship. The changes in the TEIO rainfall variability are mainly attributed to the increased SST variability over the tropical southeastern Indian Ocean, but their cause remains elusive.

KEYWORDS: Indian Ocean; Tropics; Monsoons; Rainfall; Upper troposphere; Decadal variability

1. Introduction

The upper-level tropical easterly jet (TEJ) is a strong jet stream in the Eastern Hemisphere with a maximum wind speed of roughly 35–40 $m\,s^{-1}$ over South Asia. It arises primarily from the thermal contrast between land and ocean along the southern flank of the subtropical high (Koteswaram 1958; Flohn 1964; Raghavan 1973; Nicholson and Grist 2003; Sathiyamoorthy et al. 2004). The TEJ occurs during the Indian summer monsoon season from June to September and plays an essential role in distributing climatological rainfall over the Asian and African monsoon regions. It has been found that the summer rainfall mainly locates north of the jet entrance in South Asia and south of the jet exit in western Africa (Koteswaram 1958; Flohn 1964; Webster and Fasullo 2003; Hulme and Tosdevin 1989). The TEJ variability can also exert great impact on the genesis and development of the tropical cyclones via modulating the vertical easterly shear (Rao et al. 2004; Wang et al. 2015). A weakened TEJ favors more severe tropical cyclones over the north Indian Ocean (Rao et al. 2008). Thus, investigating the variability of the TEJ is of importance for the prediction of tropical climate.

A great portion of literature has paid attention to the close connection between the TEJ and the Indian summer monsoon rainfall (ISMR). When India receives more (less) rainfall, which indicates a positive (negative) anomaly of the ISMR, the upper-tropospheric TEJ becomes stronger (weaker) (Kanamitsu et al. 1972; Tanaka 1982; Chen and Van Loon 1987; Pattanaik and Satyan 2000; Madhu 2014). Based on the close relationship between the TEJ and rainfall, it is suggested that the release of latent heat due to a large amount of rainfall in monsoon region may be critical in modulating the TEJ variability (Chen and Yen 1991; Tanaka 1982; Raghavan 1973; Lu and Ding 1989). Wang et al. (2020) suggested that convective heating associated with the midtropospheric ascent motion drives divergence in the upper troposphere and convergence in the lower troposphere, leading to the upper-level anticyclonic and lower-level cyclonic circulations. This vertical structure indicates the strengthened easterlies in the upper troposphere along the southern flank of the anticyclone and midtroposphere warming in the convective region according to the thermal wind balance. From the perspective of energetics, the convective latent heating and positive temperature anomaly generate the available potential energy, which can be converted to kinetic energy, and thus drive the large-scale tropical circulation. Sathiyamoorthy et al. (2007) found that a northward shift of the TEJ follows the intraseasonal northward propagating monsoon convective belts in South Asia by about 2 weeks due to the northward shift of the latent heat source. Rao and Srinivasan (2016) showed that a zonal shift in the

Corresponding author: Zhiping Wen, zpwen@fudan.edu.cn

DOI: 10.1175/JCLI-D-20-0631.1

© 2021 American Meteorological Society. For information regarding reuse of this content and general copyright information, consult the AMS Copyright Policy (www.ametsoc.org/PUBSReuseLicenses).

Brought to you by Peking University | Unauthenticated | Downloaded 03/24/21 03:14 AM UTC

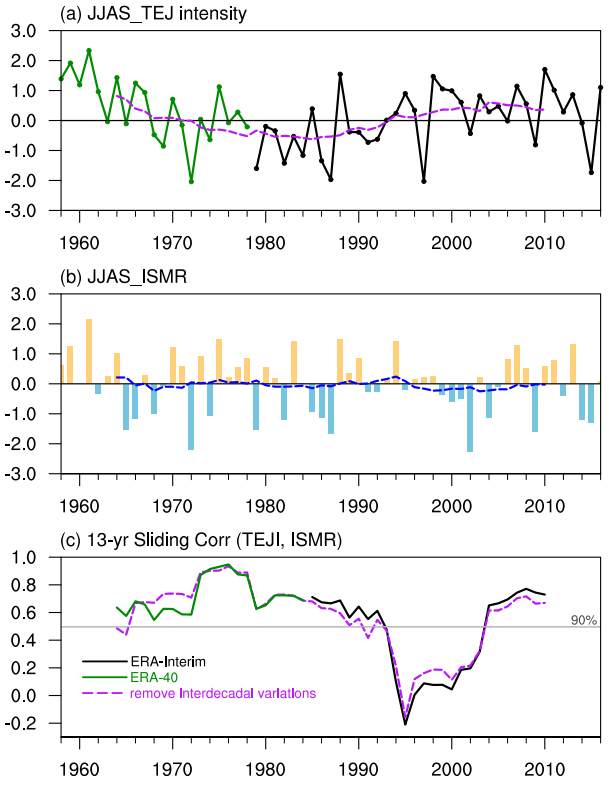

FIG. 1. Time series of normalized (a) TEJI and (b) ISMR in June–September (JJAS). The TEJI is defined as the 200-hPa zonal wind averaged over 0°–15°N, 0°–70°E and is multiplied by −1 so that a positive (negative) TEJI represents a stronger (weaker) TEJ. The ISMR is represented by the all-India rainfall (AIR) index, the total amount of JJAS rainfall averaged over all of India. The purple (blue) dashed line denotes the 13-yr running average of the TEJI (ISMR). (c) The sliding correlation coefficient between the TEJI and ISMR with a window of 13 years. The solid (dashed) line is calculated with 13-yr running average included (excluded). The black (green) line means using the ERA-Interim (ERA-40) dataset. The gray line denotes a 90% confidence level for a 13-yr correlation coefficient.

location of the rainfall leads to a similar shift in the zonal location of the TEJ and highlighted the potential role of the latent heating in determining the TEJ location. Over the exit of the TEJ in West Africa, it is also suggested that the convective rainfall is important as a key role in determining the upper-level easterly flow (Thorncroft and Blackburn 1999; Nicholson and Grist 2003).

Variations of the TEJ and the associated impacts have received increasing attention (e.g., Huang et al. 2019, 2020). Sathiyamoorthy (2005) reported a significant reduction in the intensity of the TEJ between the 1960s and 1990s, while Venkat Ratnam et al. (2013) found a sharp strengthening of the TEJ during 2001–10, indicating that interdecadal variation exists in the TEJ (Fig. 1a). The TEJ intensity has experienced an evident decline before the 1980s and an increase after the 1980s. In contrast, the ISMR shows very weak interdecadal variation (Fig. 1b). Both the TEJ and ISMR exhibit noticeable year-to-year variability, and they are significantly positively correlated during the entire period ($r = 0.57$, $p < 0.01$). When a decadal time scale is considered, the TEJ–ISMR relationship is stationary before the 1990s but undergoes an abrupt breakdown from the early1990s to the early 2000s (Fig. 1c).

Nagarjuna Rao et al. (2015) first pointed out a weakening in the TEJ–ISMR relationship in the recent three decades and attributed it to the unequal rates of decrease trends of the TEJ and ISMR in the context of the Indian Ocean warming. However, the result in Fig. 1c shows that the changes in the TEJ–ISMR relationship are highly similar before and after removing the multidecadal component by subtracting the 13-yr running average. This indicates that the trend over several decades, or interdecadal variations, can only explain a small portion of the variance associated with the weakened TEJ–ISMR relationship. It remains unclear whether the changes on other time scales, such as the interannual variability, can contribute to the weakening TEJ–ISMR relationship. This motivates us to conduct an in-depth investigation on the possible cause of the breakdown of the TEJ–ISMR relationship from the early 1990s to the early 2000s.

Section 2 details the changes in the relationship between the TEJ and ISMR. Section 3 investigates the factors that can potentially contribute to the breakdown of the TEJ–ISMR relationship. In section 4, we explore the root causes of the change in the TEJ–ISMR relationship. Section 5 provides a summary and discussion.

2. Observed decadal changes in the TEJ–ISMR relationship

The data analyzed cover the boreal summer [June–September (JJAS)] from 1979 to 2016. The monthly mean wind data are derived from the European Centre for Medium-Range Weather Forecasts (ECMWF) interim reanalysis (ERA-Interim; Simmons et al. 2007) with a horizontal resolution of 2.5° × 2.5°. The 40-Year ECMWF Re-Analysis (ERA-40; Uppala et al. 2005) is also used for 1958–2001 in Fig. 1. The monthly precipitation data are obtained from the Global Precipitation Climatology Project (GPCP; Adler et al. 2003), version 2.3. The SST data derived from the Hadley Centre Global Sea Surface Temperature (HadISST) dataset (Rayner et al. 2003) with a horizontal resolution of 1° × 1° are used to detect the forcing of SST on the rainfall variability. All the data used in the following analysis are detrended to eliminate the linear influence of the trend or interdecadal variations after 1979.

The TEJ index (TEJI) is defined as the averaged 200-hPa zonal wind over the region of 0°–15°N, 0°–70°E following Huang et al. (2019), who pointed out that the interannual variability of the TEJ mainly locates in its central-western region. In the present study the TEJI is multiplied by −1 so that a positive (negative) TEJI represents a stronger-than-normal (weaker-than-normal) TEJ.

As mentioned in section 1, it is evident that the TEJ–ISMR relationship undergoes remarkable decadal changes around the early 1990s and early 2000s (Fig. 1c). Before the early 1990s, significantly positive correlation was featured in the TEJ–ISMR relationship, followed by a dramatic decline

Brought to you by Peking University | Unauthenticated | Downloaded 03/24/21 03:14 AM UTC

around 1993/94. Their relationship becomes insignificant from the mid-1990s to the early 2000s, indicating an independent influence of the ISMR on the TEJ during that period. After 2004, the pronounced positive TEJ–ISMR relationship reappears with the correlation roughly the same as that before the early 1990s. Notably, these decadal changes of the TEJ–ISMR relationship are not sensitive to the choice of the domain that defines the TEJ at 200 or 150 hPa. However, the key region moves northward to 10°–25°N at 100 hPa as the ISMR-related zonal wind shifts northward. Our results show that the definition of the TEJI would not yield a significantly different result as long as an ISMR-related region is chosen to define the TEJI (figure not shown). It also affirms that the TEJ, which used to be related to the ISMR, becomes unrelated to the ISMR between the early 1990s and early 2000s. In addition, since the reanalysis data may underestimate the upper-level wind speed (Roja Raman et al. 2009), we also compared the observation derived from the radiosonde with the reanalysis. It is found that the reanalysis indeed underestimates the TEJ's intensity by 1–3 $m\,s^{-1}$ on the interannual time scale, but similar decadal changes in the TEJ–ISMR relationship can still be seen in observation (figure not shown), indicating the availability and reliability of the reanalysis data in describing the changes of the TEJ–ISMR relationship.

To describe the decadal changes more accurately, the whole period is divided into three epochs—1979–93 (P1; 15 years), 1994–2003 (P2; 10 years), and 2004–16 (P3; 13 years)—according to the two shifting points of the 13-yr sliding correlation coefficient in Fig. 1c. The correlation coefficient between the TEJI and ISMR is 0.70 in P1 and 0.72 in P3, both significant at the 99% confidence level, whereas it drops to 0.16 during P2. Similar results can be found in the spatial distribution of the anomalous rainfall related to the TEJI (Figs. 2b–d). During P1 and P3, a stronger TEJ corresponds to excessive rainfall covering the majority of the Indian subcontinent, coherent with the tight connection between the TEJ and ISMR. On the contrary, during P2, the rainfall anomalies are hardly statistically significant over most of the Indian subcontinent, with only a narrow area being significantly positive, revealing a broken-down relationship between the TEJ and ISMR (Fig. 2c).

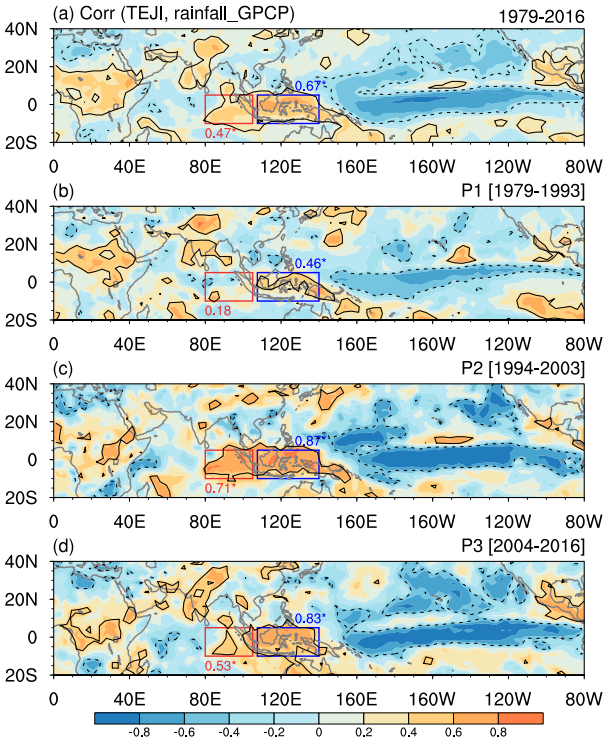

FIG. 2. Spatial distribution of the correlation coefficient between the TEJI and rainfall obtained from GPCP during (a) 1979–2016, (b) 1979–93 (P1), (c) 1994–2003 (P2), and (c) 2004–16 (P3). The contours denote the correlation coefficient significant at a 90% confidence level. The red and blue boxes represent the TEIO region (10°S–5°N, 80°–105°E) and MC region (10°S–5°N, 107.5°–140°E), respectively. The values in red and blue beside the boxes indicate the correlation coefficient between TEJI and TEIO rainfall and MC rainfall, respectively. The asterisk indicates that the correlation coefficient is significant at a 90% confidence level.

3. Why the TEJ–ISMR relationship breaks down during 1994–2003

a. Detection of contributors to the TEJ variability

A weakened TEJ–ISMR relationship during P2 indicates that the ISMR is no longer an important factor in determining the TEJ variability. To unravel the cause of the breakdown of the TEJ–ISMR relationship, we hypothesize that the TEJ fluctuation is not solely related to the ISMR. To detect the possible linkages between the TEJ and tropical rainfall in general, we examine the spatial distribution of the correlation coefficient between the interannual variation of the TEJI and tropical rainfall anomalies (Fig. 2a). In addition to the positive ISMR anomalies, the positive anomalies between 80° and 140°E and negative anomalies over tropical Pacific are observed corresponding to a stronger TEJ as well. It has been well documented that the tropical rainfall associated with the latent heat release is important in modulating the tropical circulations (e.g., Ramage 1968; Neale and Slingo 2003), indicating that the anomalous rainfall over the tropics may play important roles in the TEJ's variability. For example, Huang et al. (2020) suggested that suppressed rainfall over the tropical eastern Indian Ocean (TEIO) and Central America contributes to the weakening of the upper-level TEJ in the context of the global warming.

Since the TEJ–ISMR relationship changes on the decadal time scale, it is conceivable that the connection between the tropical rainfall and the TEJI may change similarly. Results in Figs. 2b–d show that the TEJ-related rainfall anomalies over the tropics indeed experience decadal changes. The correlations between the TEJ and rainfall over the Maritime Continent (MC; 10°S–5°N, 107.5°–140°E; blue box in Fig. 2) and tropical Pacific are generally weak during P1 but enhance evidently during P2 and remain significant during P3. It is noteworthy that the correlation over the TEIO (10°S–5°N, 80°–105°E; red box in Fig. 2) strengthens significantly during P2 but weakens during P3, which is opposite to the decadal changes of

Brought to you by Peking University | Unauthenticated | Downloaded 03/24/21 03:14 AM UTC

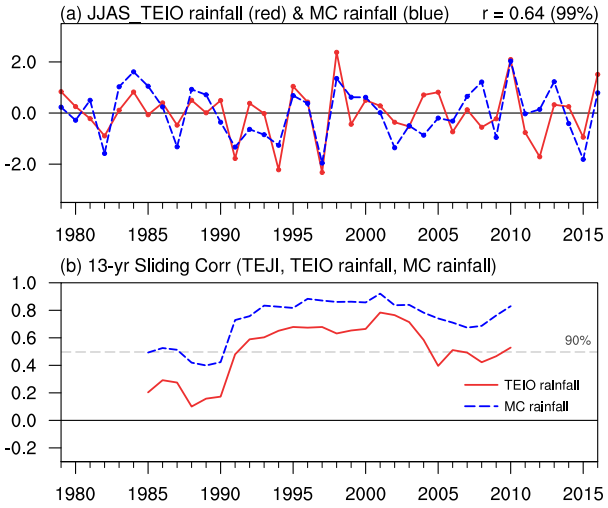

FIG. 3. (a) Time series of normalized TEIO rainfall (red) and MC rainfall (blue) in JJAS from 1979 to 2016. The correlation coefficient between the TEIO rainfall and MC rainfall is shown in the top right of the panel. (b) The sliding correlation coefficient between the TEJI and TEIO rainfall (red) and MC rainfall (blue) with a window of 13 years. The dashed line denotes a 90% confidence level for a 13-yr correlation coefficient.

the TEJ–ISMR relationship. Figure 3 compares the TEIO and MC rainfall and their correlation with the TEJ. The TEJ–TEIO rainfall relationship indeed manifests two obvious decadal changes around the early 1990s and the early 2000s, concurring with the decadal change of the TEJ–ISMR relationship, while the TEJ–MC rainfall relationship only experiences a decadal enhancement around the early 1990s (Table 1). In this case, it is very likely that the TEIO rainfall variability contributes to the breakdown of the TEJ–ISMR relationship during P2.

b. *Impacts of the TEIO rainfall on the TEJ–ISMR relationship*

The diabatic heating related to the rainfall anomalies can modify both the lower-level and upper-level circulation (Gill 1980; Matsuno 1966; Xie and Wang 1996; Wang et al. 2003). To further explore the possible influence of the TEIO rainfall in the connection between the TEJ and ISMR, Figs. 4–6 present the anomalies of rainfall, the lower-level and upper-level winds, the upper-level streamfunction, and velocity potential regressed onto the TEIO rainfall. During P1, positive rainfall anomalies are seen over the TEIO with the maximum center locating in the southern TEIO (~5°S) (Fig. 4a). The MC region also receives more rainfall while the tropical western Pacific is dominated by the suppressed rainfall anomalies. At 850 hPa, a weak C-shaped cyclonic circulation associated with the positive TEIO and MC rainfall anomalies occurs over the Bay of Bengal and the north of the TEIO (Fig. 4a). Anomalous easterlies flow westward from the tropical western Pacific and converge over the MC and TEIO region. At the upper troposphere, the corresponding atmospheric circulations mainly appear to the east of the TEIO. Specifically, a pair of weak cyclones and anticyclones locate at both sides of the equator over the western and eastern Pacific, respectively, resembling the Rossby wave responses to the negative tropical western Pacific rainfall anomalies (Figs. 4a and 5a). To the west of the TEIO, no obvious upper-level divergence over TEIO and easterlies anomalies can be found associated with the excessive TEIO rainfall (Fig. 6a), implying that the TEIO rainfall could not have an influence on the TEJ variability during P1.

Obvious intensifications in the rainfall and circulations are found during P2. The amplitudes of the positive TEIO rainfall, positive MC rainfall, and negative tropical western Pacific rainfall anomalies exhibit apparent increases (Fig. 4b). The C-shaped cyclonic circulation is evident and extends westward to the Indian subcontinent and Arabian Sea (Fig. 4b). The easterly anomalies prevail from the Bay of Bengal to central India and weaken the climatological westerly lower-level monsoon flow, leading to dry conditions over northern India. Meanwhile, the lower-level convergence of the cyclonic circulation causes the above-normal rainfall over peninsular India. Such a cyclonic circulation results in a meridional dipole-like rainfall pattern over the Indian subcontinent (Mishra et al. 2012). As a result, the total rainfall averaged over the Indian subcontinent is weak during P2, which is unfavorable for the upper-level TEJ variability and a positive TEJ–ISMR relationship. Corresponding to the increased TEIO rainfall anomalies, a pair of upper-level cyclones over the tropical western Pacific strengthens; a pair of anticyclones emerges to the west of the TEIO and straddles the equator over the Indian Ocean and Africa (Fig. 5b). Accordingly, significantly stronger easterly anomalies flow between the anticyclones to the west of TEIO. The structures of the lower- and upper-level circulations mentioned above are akin to the Rossby wave responses to the tropical heating under the background of vertical easterly shear (Xie and Wang 1996; Wang et al. 2003; Wang and Xie 1996). It suggests a possible role of the TEIO rainfall in modulating the TEJ–ISMR relationship via the Rossby wave responses at the

TABLE 1. Correlation coefficients between the TEJI, ISMR, TEIO rainfall, MC rainfall, SEIO SST, and Niño-3.4 SST during different epochs. P1, P2, and P3 denote the periods 1979–93, 1994–2003, and 2004–16, respectively. One and two asterisks (* and **) denote the correlation coefficient significant at the 90% and 95% confidence level, respectively.

	1979–2016	P1	P2	P3
Corr (TEJI, ISMR)	0.54**	0.70**	0.16	0.72**
Corr (TEJI, TEIO rainfall)	0.47**	0.18	0.71**	0.53*
Corr (TEJI, MC rainfall)	0.67**	0.46*	0.87**	0.83**
Corr (TEIO rainfall, SEIO SST)	0.73**	0.39	0.89**	0.77**
Corr (TEIO rainfall, Niño-3.4 SST)	−0.57**	−0.49*	−0.71**	−0.55*

Brought to you by Peking University | Unauthenticated | Downloaded 03/24/21 03:14 AM UTC

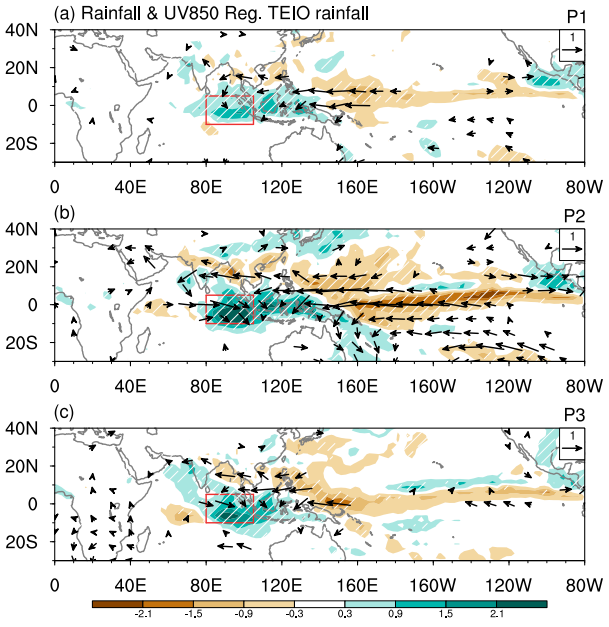

FIG. 4. Regression of the anomalous rainfall (shading; mm day^{-1}) and 850-hPa horizontal wind (vectors; m s^{-1}) onto the TEIO rainfall during (a) P1, (b) P2, and (c) P3. The white oblique lines denote significance at a 90% confidence level. Only the vectors significant at a 90% confidence level are shown. The red box represents the TEIO region (10°S–5°N, 80°–105°E).

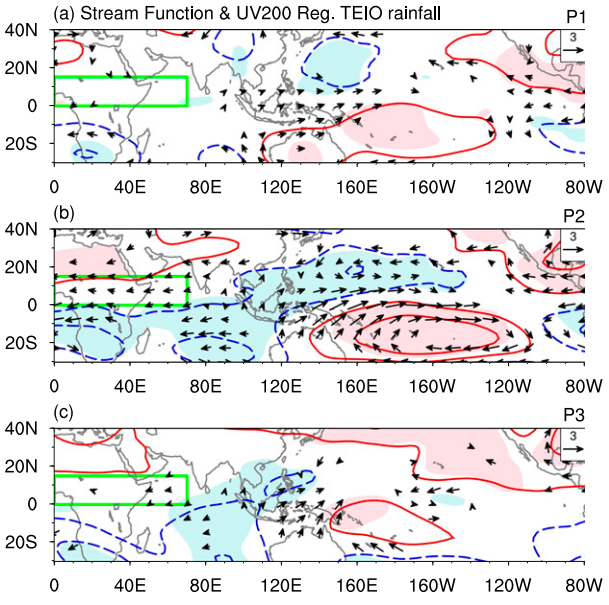

FIG. 5. As in Fig. 4, but for the 200-hPa streamfunction (contours; 10^6 m^2 s^{-1}) and 200-hPa winds (vectors; m s^{-1}). The contour interval is 2×10^6 m^2 s^{-1}. The shading denotes significance at a 90% confidence level. Only the vectors significant at a 90% confidence level are shown. The green box denotes the region of TEJI (0°–15°N, 0°–70°E).

lower- and upper-level atmospheric circulation. Additionally, the strengthened upper-level divergence over the TEIO also partly facilitates the divergent easterly winds that accelerate the TEJ (Fig. 6b). It is likely that the TEIO rainfall, along with the MC rainfall anomalies, can influence the TEJ variability much more than the ISMR during P2, as the tropical rainfall–induced lower-level circulation anomaly inhibits the impact of the Indian rainfall anomalies on the TEJ, which favors a weakened TEJ–ISMR relationship.

During P3, the amplitude of the TEIO rainfall exhibits a decrease compared to P2 (Fig. 4c), which may weaken the related lower- and upper-level circulation anomalies. The lower-level cyclonic circulation weakens and shrinks, limiting its influence on the rainfall anomalies over the Indian subcontinent (Fig. 4c). The northern anticyclone over the Indian Ocean disappears (Fig. 5c) and the upper-level divergence associated with the TEIO rainfall weakens (Fig. 6c). The weakening in the TEIO rainfall and the associated circulations indicates a weakened impact of the TEIO rainfall on the TEJ variability, in favor of the recovery of the TEJ–ISMR relationship.

The above results show that the low-level cyclonic circulation anomaly may be a key process in altering the TEJ–ISMR relationship. However, because the TEIO rainfall is related to the MC rainfall ($r = 0.64$; Fig. 3a), both TEIO rainfall and MC rainfall might be responsible for this cyclonic circulation anomaly. To distinguish the impact of TEIO rainfall and MC rainfall, partial regression analysis (Ham et al. 2013) that can remove the linear influence of each other is applied to the 850-hPa winds and rainfall. The results of partial regression analysis are displayed in Figs. 7 and 8. When the MC rainfall is excluded, the positive local convection anomaly over the TEIO itself can force a C-shaped cyclone anomaly to its north, consistent with the previous findings (Chen et al. 2018, 2019). This

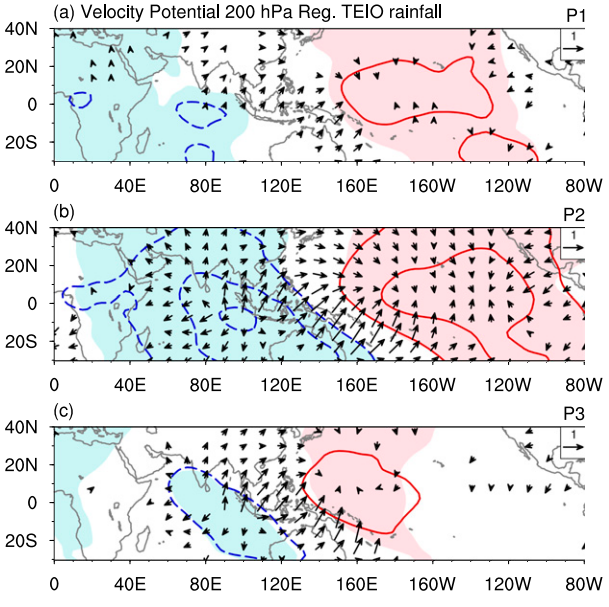

FIG. 6. As in Fig. 4, but for the 200-hPa velocity potential (contours; 10^6 m^2 s^{-1}) and divergent winds (vectors; m s^{1}). The contour interval is 0.4×10^6 m^2 s^{-1}. The shading denotes significance at a 90% confidence level. Only the vectors significant at a 90% confidence level are shown.

Brought to you by Peking University | Unauthenticated | Downloaded 03/24/21 03:14 AM UTC

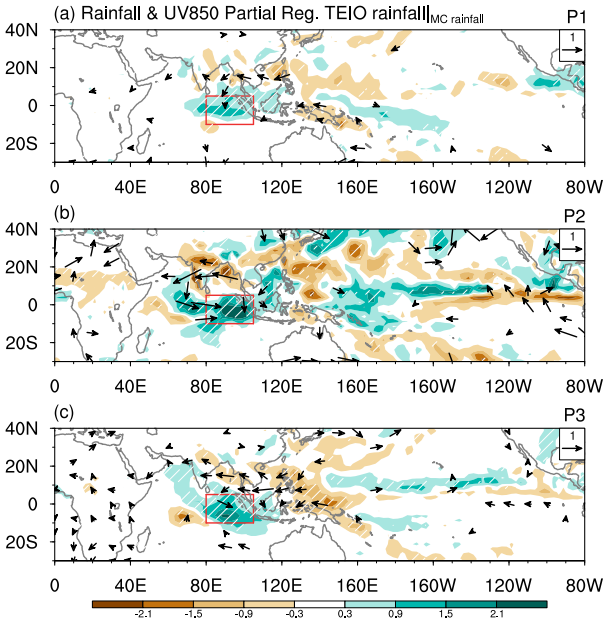

FIG. 7. Partial regression of the anomalous rainfall (shading; mm day^{-1}) and 850-hPa horizontal wind (vectors; m s^{-1}) onto the TEIO rainfall with the MC rainfall excluded during (a) P1, (b) P2, and (c) P3. The white oblique lines denote significance at a 90% confidence level. Only the vectors significant at a 90% confidence level are shown. The red box represents the TEIO region (10°S–5°N, 80°–105°E).

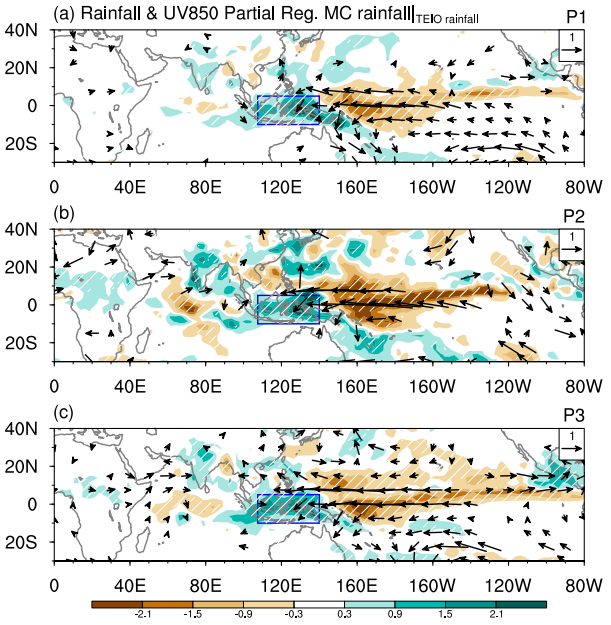

FIG. 8. As in Fig. 7, but for the MC rainfall with TEIO rainfall excluded. The blue box represents the MC region (10°S–5°N, 107.5°–140°E).

cyclonic circulation is weaker and narrow in P1 and P3 but gets stronger and broader in P2. A broader cyclonic circulation with anomalous easterly along its northern flank can weaken the climatological monsoonal westerlies flow and thus reduce the rainfall along the Ghats and northern India (Fig. 7b), which is unfavorable for the TEJ variability. In contrast, with the removal of TEIO rainfall signals, the MC rainfall shows a closer connection with the climate over the tropical Pacific in three epochs, akin to the responses to El Niño–Southern Oscillation (ENSO) cold events during boreal summer (Fig. 8). No cyclonic circulations corresponding to the MC rainfall can be found over the Indian subcontinent, but positive ISMR anomalies appear, which may be induced by the ENSO via the large-scale Walker circulation anomaly and regional Hadley circulation anomaly (Krishnamurthy and Goswami 2000). Thus, the ISMR can still influence the TEJ variability and thus maintain a positive correlation with the TEJ.

The partial correlation coefficient (Sankar-Rao et al. 1996) can further reveal the important role of the TEIO rainfall in the TEJ–ISMR relationship to some extent. If the influence of the TEIO rainfall is ruled out, the TEJ–ISMR relationship remains significantly positive during P1 ($r = 0.69$, $p < 0.01$) and P3 ($r = 0.79$, $p < 0.01$), but their correlation coefficient increases to 0.49 during P2, which is only 0.16 when including the TEIO rainfall's impact. This difference suggests that the TEJ–ISMR relationship would not experience such a dramatic drop during P2 if the TEIO rainfall has no effects on the TEJ or ISMR, which in turn confirms the role of the TEIO rainfall in interrupting the TEJ–ISMR relationship.

4. Plausible reasons for the changing TEIO rainfall variability

It has been shown that the TEIO rainfall and the associated low-level circulation are critical in modulating the TEJ–ISMR relationship. An interesting issue remains as to why the influence of the TEIO rainfall on the TEJ–ISMR relationship changes. Figure 4 has shown the evident difference in the amplitudes of the TEIO rainfall anomalies during three epochs. We hypothesize that the changes in the interannual variability of the TEIO rainfall are responsible for the resulted lower-level circulation anomaly and its influence on the TEJ–ISMR relationship. To test this assertion, we examine the changes in the amplitude of the TEIO rainfall variability by calculating the 13-yr sliding standard deviation (Fig. 9). An

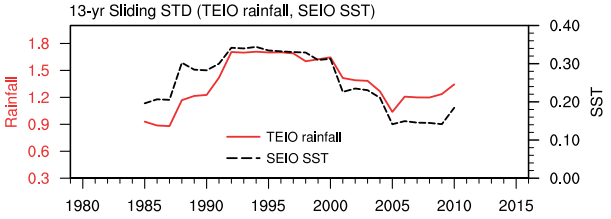

FIG. 9. The sliding standard deviation of TEIO rainfall (red; mm day^{-1}) and SEIO SST (black; °C) with a window of 13 years. The SEIO SST is defined as the averaged SST over the SEIO region (15°S–0°, 90°–110°E).

Brought to you by Peking University | Unauthenticated | Downloaded 03/24/21 03:14 AM UTC

TABLE 2. Standard deviation of the TEIO rainfall, SEIO SST, and Niño-3.4 SST during three epochs.

	P1	P2	P3
TEIO rainfall (mm day^{-1})	0.87	1.81	1.34
SEIO SST (°C)	0.21	0.35	0.18
Niño-3.4 SST (°C)	0.67	0.67	0.68

obvious increase and a decrease of the amplitude of the TEIO rainfall variability can be found in the early 1990s and early 2000s, respectively (red solid line in Fig. 9), coherent with the changes in the TEJ–ISMR relationship as well as the TEJ–TEIO rainfall relationship. During P1, the magnitude of the TEIO rainfall is only 0.87 mm day^{-1} during P1, but it becomes nearly double (1.81 mm day^{-1}) during P2 (Table 2). The intensified rainfall variability may exert stronger and more significant impacts on the atmospheric circulations. This helps explain how a stronger and broader lower-level cyclonic circulation and stronger upper-level circulation responded, which is conducive to the breakdown of the TEJ–ISMR relationship during P2. The magnitude of the TEIO rainfall variability drops to 1.34 mm day^{-1} during P3, resulting in a weakened impact on the TEJ and favoring a positive TEJ–ISMR relationship.

The change in the amplitude of the rainfall variability is likely owing to the change in the SST variability. Figure 10 displays the spatial distribution of the simultaneous SST regressed on the TEIO rainfall. It is found that the interannual variation of the TEIO rainfall is significantly related to the local SST anomalies, that is, the tropical southeastern Indian Ocean (SEIO; 15°S–0°, 90°–110°E) during P2 ($r = 0.89$, $p < 0.01$) while their relationship decreases during P3 ($r = 0.77$, $p < 0.01$) and almost disappears during P1 ($r = 0.39$, $p > 0.1$). Consistent with the changes in the TEIO rainfall variability, the SEIO SST variability also experiences two decadal changes in the early 1990s and early 2000s (black dashed line in Fig. 9). The variability of the SEIO SST shows the strongest amplitude during P2 (0.35°C) and smaller ones during P1 (0.21°C) and P3 (0.18°C). Chen et al. (2019) demonstrated that SEIO warming can induce local convective heating in both observational data and numerical experiments, which triggers lower-level C-shaped wind anomalies that affect the climate over the Indian Ocean section. The strengthened SEIO SST variability during P2 can facilitate enhanced TEIO rainfall anomalies, helping the TEIO rainfall exert influences on the TEJ variability and modulate the TEJ–ISMR relationship. This result is consistent with the results of Chen et al. (2017). They found an increase in the amplitude of the tropical eastern Indian Ocean SST variability after the early 1990s, which is conducive to the intensified interannual variability of the southern China summer rainfall through changing the local meridional vertical circulation.

It is reported that the impact of the tropical Pacific via the atmospheric bridge is discernable (e.g., Lau and Nath 1996; Klein et al. 1999; Wang 2002; Chiang and Lintner 2005). The cause of the excessive TEIO rainfall may be related to the remote forcing from Pacific ENSO. Figure 10 illustrates a cooling over the tropical central-eastern Pacific (Niño-3.4 region; 5°S–5°N, 170°–120°W) corresponding to the excessive TEIO rainfall. The cooling pattern over the Niño-3.4 region is relatively weak during P1 but strengthens during P2 (Figs. 10a,b), concurring with the intensified relationship between the TEIO rainfall and the Niño-3.4 index ($r = -0.49$ in P1 and $r = -0.71$ in P2). Note that the variance of the Niño-3.4 SST does not show any decadal changes (Table 2). A closer TEIO rainfall–Niño-3.4 SST relationship during P2 may indicate an enhanced impact of the Pacific ENSO on the TEIO rainfall via inducing an anomalous Walker circulation in the Indo-Pacific region and maintaining the upper-level divergence over the Indian Ocean (Fig. 6b), which contributes to the enhancement of the TEIO rainfall variability. As the tropical central-eastern Pacific cooling weakens during P3 (Fig. 10c), the correlation coefficient between the TEIO rainfall and Niño-3.4 SST decrease to −0.55, suggesting a weakened impact of the ENSO on the TEIO rainfall variability.

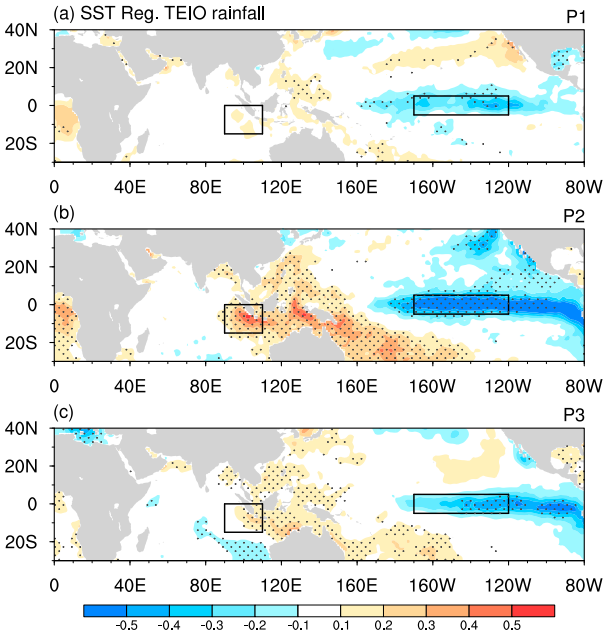

FIG. 10. Regression of the anomalous SST (shading; °C) onto the TEIO rainfall during (a) P1, (b) P2, and (c) P3. The dots denote significance at a 90% confidence level. The boxes represent the SEIO region (15°S–0°, 90°–110°E) and Niño-3.4 region (5°S–5°N, 170°–120°W).

5. Summary and discussion

The TEJ and ISMR are prominent features of the Asian summer monsoon system and exhibit a positive correlation. Using the reanalysis data from 1979 to 2016, the present study demonstrates that the TEJ–ISMR relationship has experienced two abrupt decadal changes, one in the early 1990s and the other in the early 2000s. The TEJ is significantly positively related to the ISMR except during 1994–2003 when this relationship is broken down. We find that TEIO rainfall variability plays a vital role in modulating the TEJ–ISMR relationship.

Brought to you by Peking University | Unauthenticated | Downloaded 03/24/21 03:14 AM UTC

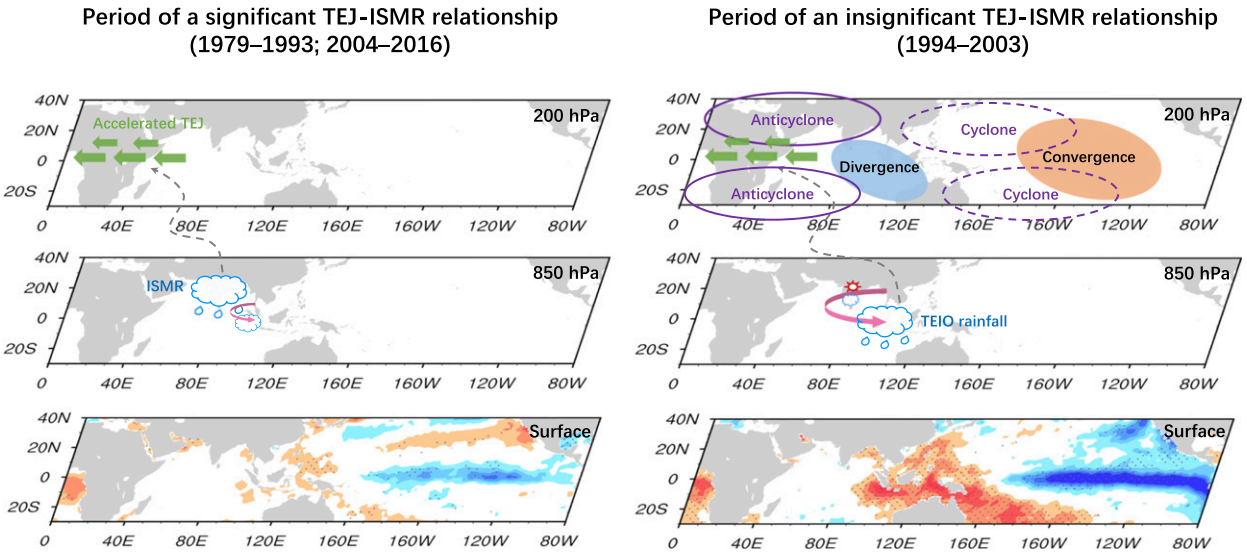

FIG. 11. Schematic diagram of the role of the TEIO rainfall in the interdecadal changes of the TEJ–ISMR relationship. The green vectors indicate the intensified TEJ at 200 hPa. The purple solid (dashed) circle represents the anticyclones (cyclones). The blue (orange) shading represents the divergent (convergent) center. The cloud (sun) marker represents excessive (deficient) rainfall. The pink arc-shaped vector indicates the C-shaped cyclone anomaly induced by the TEIO rainfall. The gray dashed curves indicate the main process by which the TEJ is influenced by the rainfall. (bottom) The TEIO rainfall-related SST anomalies.

Both the TEJ–TEIO rainfall relationship and the TEIO rainfall variability have experienced two similar shifts in the early 1990s and early 2000s with enhanced TEJ–TEIO rainfall relationship and TEIO rainfall variability during 1994–2003. It indicates that when the TEIO rainfall variability enhances, the ISMR tends to weaken, and the contribution of the TEIO rainfall to the TEJ variability can dominate and break down the TEJ–ISMR relationship.

Figure 11 summarizes the processes by which TEIO rainfall modulates the TEJ–ISMR relationship during different epochs. When the TEIO rainfall fluctuates in a relatively small amplitude during 1979–93 and 2004–16 (left panel in Fig. 11), the TEIO rainfall-induced lower-level cyclonic circulation is narrow, and the associated upper-level circulations over the Indian Ocean are weak, which have a negligible influence on the TEJ and ISMR variations as well as the TEJ–ISMR relationship. In contrast, when the TEIO rainfall variability increases during 1994–2003 (right panel in Fig. 11), the TEIO rainfall-induced lower-level cyclonic circulation is strong and extends westward to the Arabian Sea, causing reduced ISMR; meanwhile, it excites a pair of upper-level anticyclones and upper-level divergent winds, both strengthening the upper-level TEJ significantly. Thus, the enhanced TEIO rainfall variability, taking the place of the ISMR, plays a more critical role in the TEJ variability and thus contributes to the breakdown of the TEJ–ISMR relationship.

The changes in the TEIO rainfall variability can be mainly attributed to the increased SST variability over the SEIO. Additionally, a closer relationship between the TEIO rainfall and Niño-3.4 SST during 1994–2003 also indicates the contribution of the Pacific ENSO to the increase of the TEIO rainfall variability.

The relationship between the TEIO rainfall, SEIO SST, and Niño-3.4 SST are all in phase on the decadal time scale. An issue here is what the root cause of the TEIO rainfall variability is: the remote forcing from ENSO or local SST anomalies over the SEIO? Figure 10 indicates that TEIO rainfall is positively correlated with SEIO SST anomalies, suggesting that the local SST anomalies can be viewed as a direct driver for the TEIO rainfall (Wang et al. 2004, 2005). However, the SEIO SST anomalies may be remotely triggered by ENSO and significantly amplified by the local atmosphere–ocean interaction in the southern Indian Ocean (Wang et al. 2003). In this sense, ENSO could play a role in the SST variability over the SEIO. Due to the interactive nature of the atmosphere–ocean system, it is difficult to isolate the relative contribution of ENSO through the Walker cell or through triggering the Indian Ocean atmosphere–ocean interaction. The latter can amplify both the SST and rainfall anomalies over the tropical eastern Indian Ocean. This should be addressed in future work.

The present study considers the TEJ as the response to the forcing, Indian rainfall. In fact, the TEJ can also influence the rainfall via, for example, the upper-level divergence (Nicholson and Grist 2003), vertical easterly shear (Rao et al. 2008), interaction with the African easterly wave activity (Grist et al. 2002), and modulation of the equatorial Rossby wave activity (Yang et al. 2018). It comes naturally that decadal changes in the TEJ may lead to the changes in the TEJ–ISMR relationship. However, the variability and the structure of the TEJ do not exhibit obvious decadal changes (figure not shown). It seems that the contributor of the breakdown of the TEJ–ISMR relationship comes from the change in the rainfall anomalies.

The present study focuses on the seasonal-mean TEJ–ISMR relationship. As the Indian rainfall and its relationship with the

Brought to you by Peking University | Unauthenticated | Downloaded 03/24/21 03:14 AM UTC

TEJ may vary month by month, whether TEIO rainfall can influence the monthly TEJ–ISMR relationship is still unknown. We compared the monthly correlation coefficient between the TEJ and ISMR and TEIO rainfall from June to September during different epochs. It is found that only during P2 when the JJAS-averaged TEJ–ISMR relationship is weakened, the TEJ–ISMR relationship exhibits a large variation, likely influenced by the TEIO rainfall via a similar way mentioned in the present study (figure not shown). When JJAS-averaged TEJ is significantly related to the ISMR, the TEJ–ISMR relationship variation is small and the influence of the TEIO rainfall can be ignored. This provides another aspect to understand the change of the TEJ–ISMR relationship and further confirm the role of the TEIO rainfall on the TEJ–ISMR relationship.

Acknowledgments. The authors sincerely thank the three anonymous reviewers for their constructive suggestions. This research is jointly supported by National Key Research and Development Program of China (2016YFA0600601), National Natural Science Foundation of China (41530530, 41875087, 41805057), the Guangdong Natural Science Foundation (2018A030310023), and the Southern Marine Science and Engineering Guangdong Laboratory (Guangzhou) (GML2019ZD0306). BW acknowledges the support from the NSF/Climate Dynamics Award AGS-1540783. This is the International Pacific Research Center (IPRC) Publication No. 1498, the School of Ocean and Earth Science and Technology (SOEST) Publication No. 11224, and Earth System Modeling Center (ESMC) Publication No. 341.

REFERENCES

Adler, R. F., and Coauthors, 2003: The version-2 Global Precipitation Climatology Project (GPCP) monthly precipitation analysis (1979–present). *J. Hydrometeor.*, **4**, 1147–1167, https://doi.org/10.1175/1525-7541(2003)004<1147:TVGPCP>2.0.CO;2.

Chen, J., Z. Wen, R. Wu, X. Wang, C. He, and Z. Chen, 2017: An interdecadal change in the intensity of interannual variability in summer rainfall over southern China around early 1990s. *Climate Dyn.*, **48**, 191–207, https://doi.org/10.1007/s00382-016-3069-8.

Chen, T., and H. Van Loon, 1987: Interannual variation of the tropical easterly jet. *Mon. Wea. Rev.*, **115**, 1739–1759, https://doi.org/10.1175/1520-0493(1987)115<1739:IVOTTE>2.0.CO;2.

——, and M. Yen, 1991: Intraseasonal variations of the tropical easterly jet during the 1979 northern summer. *Tellus*, **43A**, 213–225, https://doi.org/10.3402/tellusa.v43i3.11928.

Chen, Z., Y. Du, Z. Wen, R. Wu, and C. Wang, 2018: Indo-Pacific climate during the decaying phase of the 2015/16 El Niño: Role of southeast tropical Indian Ocean warming. *Climate Dyn.*, **50**, 4707–4719, https://doi.org/10.1007/s00382-017-3899-z.

——, ——, ——, ——, and S. P. Xie, 2019: Evolution of south tropical Indian Ocean warming and the climatic impacts following strong El Niño events. *J. Climate*, **32**, 7329–7347, https://doi.org/10.1175/JCLI-D-18-0704.1.

Chiang, J. C. H., and B. R. Lintner, 2005: Mechanisms of remote tropical surface warming during El Niño. *J. Climate*, **18**, 4130–4149, https://doi.org/10.1175/JCLI3529.1.

Flohn, H., 1964: Investigations on the tropical easterly jet. Bonner Meteorology Abhandlungen, 83 pp., https://www2.meteo.uni-bonn.de/bibliothek/Flohn_Publikationen/K141-K190_1959-1965/K176.pdf.

Gill, A. E., 1980: Some simple solutions for heat induced tropical circulation. *Quart. J. Roy. Meteor. Soc.*, **106**, 447–462, https://doi.org/10.1002/qj.49710644905.

Grist, J. P., S. E. Nicholson, and A. I. Barcilon, 2002: Easterly waves over Africa. Part II: Observed and modeled contrasts between wet and dry years. *Mon. Wea. Rev.*, **130**, 212–225, https://doi.org/10.1175/1520-0493(2002)130<0212:EWOAPI>2.0.CO;2.

Ham, Y.-G., J.-S. Kug, J.-Y. Park, and F.-F. Jin, 2013: Sea surface temperature in the north tropical Atlantic as a trigger for El Niño/Southern Oscillation events. *Nat. Geosci.*, **6**, 112–116, https://doi.org/10.1038/ngeo1686.

Huang, S., Z. Wen, Z. Chen, X. Li, R. Chen, and Y. Guo, 2019: Interdecadal change in the relationship between the tropical easterly jet and tropical sea surface temperature anomalies in boreal summer. *Climate Dyn.*, **53**, 2119–2131, https://doi.org/10.1007/s00382-019-04801-5.

——, B. Wang, and Z. Wen, 2020: Dramatic weakening of the tropical easterly jet projected by CMIP6 models. *J. Climate*, **33**, 8439–8455, https://doi.org/10.1175/JCLI-D-19-1002.1.

Hulme, M., and N. Tosdevin, 1989: The tropical easterly jet and Sudan rainfall: A review. *Theor. Appl. Climatol.*, **39**, 179–187, https://doi.org/10.1007/BF00867945.

Kanamitsu, M., T. N. Krishnamurti, and C. Depradine, 1972: On scale interactions in the tropics during northern summer. *J. Atmos. Sci.*, **29**, 698–706, https://doi.org/10.1175/1520-0469(1972)029<0698:OSIITT>2.0.CO;2.

Klein, S. A., B. J. Soden, and N.-C. Lau, 1999: Remote sea surface temperature variations during ENSO: Evidence for a tropical atmospheric bridge. *J. Climate*, **12**, 917–932, https://doi.org/10.1175/1520-0442(1999)012<0917:RSSTVD>2.0.CO;2.

Koteswaram, P., 1958: The easterly jet stream in the tropics. *Tellus*, **10**, 43–57, https://doi.org/10.3402/tellusa.v10i1.9220.

Krishnamurthy, V., and B. N. Goswami, 2000: Indian monsoon–ENSO relationship on interdecadal timescale. *J. Climate*, **13**, 579–595, https://doi.org/10.1175/1520-0442(2000)013<0579:IMEROI>2.0.CO;2.

Lau, N.-C., and M. J. Nath, 1996: The role of the "atmospheric bridge" in linking tropical Pacific ENSO events to extratropical SST anomalies. *J. Climate*, **9**, 2036–2057, https://doi.org/10.1175/1520-0442(1996)009<2036:TROTBI>2.0.CO;2.

Lu, J., and Y. Ding, 1989: Climatic study on the summer tropical easterly jet at 200 hPa. *Adv. Atmos. Sci.*, **6**, 215–226, https://doi.org/10.1007/BF02658017.

Madhu, V., 2014: Variation of zonal winds in the upper troposphere and lower stratosphere in association with deficient and excess Indian summer monsoon scenario. *Atmos. Climate Sci.*, **04**, 685–695, https://doi.org/10.4236/acs.2014.44062.

Matsuno, T., 1966: Quasi-geostrophic motions in the equatorial area. *J. Meteor. Soc. Japan*, **44**, 25–43, https://doi.org/10.2151/JMSJ1965.44.1_25.

Mishra, V., B. V. Smoliak, D. P. Lettenmaier, and J. M. Wallace, 2012: A prominent pattern of year-to-year variability in Indian summer monsoon rainfall. *Proc. Natl. Acad. Sci. USA*, **109**, 7213–7217, https://doi.org/10.1073/pnas.1119150109.

Nagarjuna Rao, D., G. George, C. T. Sabeerali, D. A. Ramu, and S. A. Rao, 2015: Changing relationship between the tropical easterly jet and the Indian summer monsoon rainfall: Role of Indian Ocean warming. *Indian J. Geo-Mar. Sci.*, **44**, 1678–1683.

Neale, R., and J. Slingo, 2003: The Maritime Continent and its role in the global climate: A GCM study. *J. Climate*,

Brought to you by Peking University | Unauthenticated | Downloaded 03/24/21 03:14 AM UTC

16, 834–848, https://doi.org/10.1175/1520-0442(2003)016<0834:TMCAIR>2.0.CO;2.

Nicholson, S. E., and J. P. Grist, 2003: The seasonal evolution of the atmospheric circulation over West Africa and equatorial Africa. *J. Climate*, **16**, 1013–1030, https://doi.org/10.1175/1520-0442(2003)016<1013:TSEOTA>2.0.CO;2.

Pattanaik, D. R., and V. Satyan, 2000: Fluctuations of tropical easterly jet during contrasting monsoons over India: A GCM study. *Meteor. Atmos. Phys.*, **75**, 51–60, https://doi.org/10.1007/s007030070015.

Raghavan, K., 1973: Tibetan anticyclone and tropical easterly jet. *Pure Appl. Geophys.*, **110**, 2130–2142, https://doi.org/10.1007/BF00876576.

Ramage, C. S., 1968: Role of a tropical "Maritime Continent" in the atmospheric circulation. *Mon. Wea. Rev.*, **96**, 365–370, https://doi.org/10.1175/1520-0493(1968)096<0365:ROATMC>2.0.CO;2.

Rao, B. R. S., D. V. B. Rao, and V. B. Rao, 2004: Decreasing trend in the strength of tropical easterly jet during the Asian summer monsoon season and the number of tropical cyclonic systems over Bay of Bengal. *Geophys. Res. Lett.*, **31**, L14103, https://doi.org/10.1029/2004GL019817.

Rao, S., and J. Srinivasan, 2016: The impact of latent heating on the location and strength of the tropical easterly jet. *Meteor. Atmos. Phys.*, **128**, 247–261, https://doi.org/10.1007/s00703-015-0407-z.

Rao, V. B., C. C. Ferreira, S. H. Franchito, and S. S. V. S. Ramakrishna, 2008: In a changing climate weakening tropical easterly jet induces more violent tropical storms over the north Indian Ocean. *Geophys. Res. Lett.*, **35**, L15710, https://doi.org/10.1029/2008GL034729.

Rayner, N. A., D. E. Parker, E. B. Horton, C. K. Folland, L. V. Alexander, D. P. Rowell, E. C. Kent, and A. Kaplan, 2003: Global analyses of sea surface temperature, sea ice, and night marine air temperature since the late nineteenth century. *J. Geophys. Res.*, **108**, 4407, https://doi.org/10.1029/2002JD002670.

Roja Raman, M., V. V. M. Jagannadha Rao, M. Venkat Ratnam, M. Rajeevan, S. V. B. Rao, D. Narayana Rao, and N. Prabhakara Rao, 2009: Characteristics of the tropical easterly jet: Long-term trends and their features during active and break monsoon phases. *J. Geophys. Res.*, **114**, D19105, https://doi.org/10.1029/2009JD012065.

Sankar-Rao, M., K. M. Lau, and S. Yang, 1996: On the relationship between Eurasian snow cover and the Asian summer monsoon. *Int. J. Climatol.*, **16**, 605–616, https://doi.org/10.1002/(SICI)1097-0088(199606)16:6<605::AID-JOC41>3.0.CO;2-P.

Sathiyamoorthy, V., 2005: Large scale reduction in the size of the tropical easterly jet. *Geophys. Res. Lett.*, **32**, L14802, https://doi.org/10.1029/2005GL022956.

——, P. K. Pal, and P. C. Joshi, 2004: Influence of the upper-tropospheric wind shear upon cloud radiative forcing in the Asian monsoon region. *J. Climate*, **17**, 2725–2735, https://doi.org/10.1175/1520-0442(2004)017<2725:IOTUWS>2.0.CO;2.

——, ——, and ——, 2007: Intraseasonal variability of the tropical easterly jet. *Meteor. Atmos. Phys.*, **96**, 305–316, https://doi.org/10.1007/s00703-006-0214-7.

Simmons, A., S. Uppala, D. Dee, and S. Kobayashi, 2007: ERA-Interim: New ECMWF reanalysis products from 1989 onwards. *ECMWF Newsletter*, No. 110, ECMWF, Reading, United Kingdom, 25–35, https://www.ecmwf.int/sites/default/files/elibrary/2006/14615-newsletter-no110-winter-200607.pdf.

Tanaka, M., 1982: Interannual the fluctuations of the tropical easterly monsoon in the Asian region. *J. Meteor. Soc. Japan*, **60**, 865–875, https://doi.org/10.2151/jmsj1965.60.3_865.

Thorncroft, C. D., and M. Blackburn, 1999: Maintenance of the African easterly jet. *Quart. J. Roy. Meteor. Soc.*, **125**, 763–786, https://doi.org/10.1002/QJ.49712555502.

Uppala, S. M., and Coauthors, 2005: The ERA-40 Re-Analysis. *Quart. J. Roy. Meteor. Soc.*, **131**, 2961–3012, https://doi.org/10.1256/qj.04.176.

Venkat Ratnam, M., B. V. K. Murthy, and A. Jayaraman, 2013: Is the trend in TEJ reversing over the Indian subcontinent? *Geophys. Res. Lett.*, **40**, 3446–3449, https://doi.org/10.1002/grl.50519.

Wang, B., and X. Xie, 1996: Low-frequency equatorial waves in vertically sheared zonal flow. Part I: Stable waves. *J. Atmos. Sci.*, **53**, 449–467, https://doi.org/10.1175/1520-0469(1996)053<0449:LFEWIV>2.0.CO;2.

——, R. Wu, and T. Li, 2003: Atmosphere–warm ocean interaction and its impacts on Asian-Australian monsoon variation. *J. Climate*, **16**, 1195–1211, https://doi.org/10.1175/1520-0442(2003)16<1195:AOIAII>2.0.CO;2.

——, I. S. Kang, and J. Y. Lee, 2004: Ensemble simulations of Asian-Australian monsoon variability by 11 AGCMs. *J. Climate*, **17**, 803–818, https://doi.org/10.1175/1520-0442(2004)017<0803:ESOAMV>2.0.CO;2.

——, Q. Ding, X. Fu, I. S. Kang, K. Jin, J. Shukla, and F. Doblas-Reyes, 2005: Fundamental challenge in simulation and prediction of summer monsoon rainfall. *Geophys. Res. Lett.*, **32**, L15711, https://doi.org/10.1029/2005GL022734.

——, C. Jin, and J. Liu, 2020: Understanding future change of global monsoons projected by CMIP6 models. *J. Climate*, **33**, 6471–6489, https://doi.org/10.1175/JCLI-D-19-0993.1.

Wang, C., 2002: Atmospheric circulation cells associated with the El Niño–Southern Oscillation. *J. Climate*, **15**, 399–419, https://doi.org/10.1175/1520-0442(2002)015<0399:ACCAWT>2.0.CO;2.

Wang, Z., A. Duan, and C. Li, 2015: Effect of easterly jet on formation of initial vortex of tropical cyclone Nargis over Bay of Bengal. *Trans. Atmos. Sci.*, **38**, 1–8.

Webster, P. J., and J. Fasullo, 2003: Monsoon: Dynamical theory. *Encycl. Atmos. Sci.*, **3**, 1370–1386, https://doi.org/10.1016/B0-12-227090-8/00236-0.

Xie, X., and B. Wang, 1996: Low-frequency equatorial waves in vertically sheared zonal flow. Part II: Unstable waves. *J. Atmos. Sci.*, **53**, 3589–3605, https://doi.org/10.1175/1520-0469(1996)053<3589:LFEWIV>2.0.CO;2.

Yang, G. Y., J. Methven, S. Woolnough, K. Hodges, and B. Hoskins, 2018: Linking African easterly wave activity with equatorial waves and the influence of Rossby waves from the Southern Hemisphere. *J. Atmos. Sci.*, **75**, 1783–1809, https://doi.org/10.1175/JAS-D-17-0184.1.

Brought to you by Peking University | Unauthenticated | Downloaded 03/24/21 03:14 AM UTC